JOURNAL OF GEOPHYSICAL RESEARCH, VOL. 100, NO. B7, PAGES 9921–9934, JUNE 10, 1995

Geodesy using the Global Positioning System: The effects of signal scattering on estimates of site position

P. Elósegui,[1] J. L. Davis,[1] R. T. K. Jaldehag,[2] J. M. Johansson,[2] A. E. Niell,[3] and I. I. Shapiro[1]

Abstract. Analysis of Global Positioning System (GPS) data from two sites separated by a horizontal distance of only ~2.2 m yielded phase residuals exhibiting a systematic elevation angle dependence. One of the two GPS antennas was mounted on an ~1-m-high concrete pillar, and the other was mounted on a standard wooden tripod. We performed elevation angle cutoff tests with these data and established that the estimate of the vertical coordinate of site position was sensitive to the minimum elevation angle (elevation cutoff) of the data analyzed. For example, the estimate of the vertical coordinate of site position changed by 9.7±0.8 mm when the minimum elevation angle was increased from 10° to 25°. We performed simulations based on a simple (ray tracing) multipath model with a single horizontal reflector which demonstrated that the results from the elevation angle cutoff tests and the pattern of the residuals versus elevation angle could be qualitatively reproduced if the reflector were located 0.1–0.2 m beneath the antenna phase center. We therefore hypothesized that the elevation-angle-dependent error was caused by scattering from the horizontal surface of the pillar, located a distance of ~0.2 m beneath the antenna phase center. We tested this hypothesis by placing microwave absorbing material between the antenna and the pillar in a number of configurations and by analyzing the changes in apparent position of the antenna. The results indicate that (1) the horizontal surface of the pillar is indeed the main scatterer, (2) both the concrete and the metal plate embedded in the pillar are significant sources of scattering, and (3) the scattering can be reduced greatly by the use of microwave absorbing materials. These results have significant implications for the accuracy of global GPS geodetic tracking networks which use pillar-antenna configurations identical or similar to the one used for this study at the Westford WFRD GPS site.

Introduction

Surveying with the NAVSTAR Global Positioning System (GPS) is a technique of increasingly widespread utility in civil and scientific applications requiring position, velocity, and acceleration determinations and time synchronization. First put into widespread use in the mid-1980s, GPS is the latest of the so-called space geodetic techniques and can already compete in accuracy at all terrestrial spatial scales (station separation ≤ 12,000 km) with the other techniques: very long baseline interferometry (VLBI) and satellite laser ranging (SLR). The demonstrated repeatability of horizontal position estimates obtained from GPS data is currently at the 1- to 2-mm level on local and regional scales (≤ 500 km) and is approaching, if it has not attained, the 10-mm level on global scales [e.g., *Dixon*, 1991; *Blewitt*, 1993]. Typical values for the vertical baseline component repeatability are a factor of 3–5 greater. The improvement in repeatability during the last decade has been obtained by filling out the satellite constellation and by establishing global permanent GPS networks for continuous satellite tracking and orbit determination. These advances have triggered the introduction around the world of continuously operating GPS arrays on local, regional, and global scales for studying a wide range of geophysical phenomena.

The Global Positioning System consists of a constellation of 22 satellites, plus three active spares, in nearly circular orbits, distributed in six distinct orbital planes having inclinations close to 55°. (At the time, several had inclinations of 62°.) The orbital radii of the satellites are ~26,000 km, giving them a period of 12 hours, so that the same configuration relative to the Earth occurs once every sidereal day. Each GPS satellite trans-

[1]Harvard-Smithsonian Center for Astrophysics, Cambridge, Massachusetts.
[2]Onsala Space Observatory, Chalmers University of Technology, Onsala, Sweden.
[3]Haystack Observatory, Massachusetts Institute of Technology, Westford, Massachusetts.

Paper number 95JB00868.
0148-0227/95/95JB-00868$05.00

mits highly coherent radio signals with right-hand circular polarization (RCP) over two L-band channels, L1 (1575.42 MHz) and L2 (1227.60 MHz). The L1 carrier signal is modulated by two pseudo-random noise (PRN) sequences, called the precision (P) code (10.23 MHz) and the coarse/acquisition (C/A) code (1.023 MHz), whereas the L2 signal is modulated by the P code only. The three signals are modulated, in turn, by a 50-Hz data stream which contains the satellites' ephemeris and health, clock biases, ionospheric propagation correction data, and other useful information. All of the transmitted signals are governed by an onboard atomic clock. Geodetic GPS receivers are typically capable of observing 8 to 12 GPS satellites simultaneously. Additional details concerning the Global Positioning System were presented by *Dixon* [1991] and *Blewitt* [1993].

There are two main GPS observation types: the pseudorange (P code) and the carrier beat phase (or just "phase"). The statistical error of the latter is about 1000-fold smaller than that of the former. For geodetic positioning applications, therefore, the basic observable is the carrier beat phase, which is the difference between the phase of the signal received by the ground-based GPS antenna/receiver system from a given satellite and a signal of the appropriate frequency generated by the internal oscillator of the GPS receiver. The phase is determined independently for each channel, L1 and L2. The phase observable ϕ_i for the ith frequency channel ($i = 1$ for L1 and $i = 2$ for L2) can thus be expressed (in cycles), at some epoch t [e.g., *King et al.*, 1985] as

$$\phi_i = \frac{\rho}{\lambda_i} + C_i^{\mathrm{rec}} - C_i^{\mathrm{sat}} + \phi^{\mathrm{atm}} - \phi_i^{\mathrm{ion}} - \phi_i^{\mathrm{apr}} + N + \epsilon_i \quad (1)$$

where ρ is the instantaneous distance between the receiving antenna and satellite, λ_i is the wavelength associated with the ith channel, C_i^{rec} is the receiver "clock" phase error due mainly to drifting of the receiver frequency standard from the nominal frequency, C_i^{sat} is the satellite "clock" phase error due to the same problem in the transmitting satellite, ϕ^{atm} is the phase delay due to the neutral atmosphere (nondispersive up to frequencies close to 60 GHz; see, for example, *Liebe* [1985]), ϕ_i^{ion} is the dispersive ionospheric phase delay, ϕ^{apr} is the a priori phase difference between the initial phases of the satellite and the receiver, N is an integer cycle bias or "ambiguity," and ϵ_i is the phase measurement error, random and otherwise, due to other sources (see below). In (1), all the phase quantities are expressed in units of cycles. The less precise pseudorange code observation equation is comparable to that of the phase equation except for the initial cycle ambiguity term and for the sign of the ionospheric term.

The satellite and receiver "clock" errors are easily and accurately dealt with using the method of double differencing, or its equivalent [e.g., *Counselman and Shapiro*, 1979; *Wells et al.*, 1986], which uses between-station and between-satellite differences to estimate these quantities. The ionospheric phase delay is estimated by combining the phase observables from the two frequencies [e.g., *Spilker*, 1978]. Such a combined observable will here be referred to as the "linear combination," or "LC," observable. The LC observations from multiple sites, satellites, and epochs are combined to estimate a number of parameters, including the integer ambiguities for all the site/satellite combinations, zenith atmospheric propagation delays, site positions, satellite orbital parameters, and other relevant parameters.

The main goal of this work is to study the effects of carrier-phase signal scattering on geodetic estimates of site position obtained from GPS data. Signals scattered (and reflected) from objects in the environment of the GPS antenna will interfere with the unscattered signal and thus will contribute to the measured phase to an extent which depends on the lengths of the paths traveled by the unscattered and scattered signals from their origin to the receiving antenna, and on their relative amplitudes. Both the carrier phase and the pseudo-range coded signals can suffer, though differently, from these effects. In general, the estimates of positions obtained from scattering-contaminated GPS carrier-phase and/or pseudo-range observations will be in error.

The term multipath is used in the GPS literature to refer to the reflected signal. It is implicit in this terminology that the reflecting structure is located in the far field of the antenna. In this zone the shape of the antenna field pattern is independent of the distance, and therefore its electromagnetic properties are not affected by the presence of reflectors. Geometrical ray optics is then usually adequate in describing the multipath effect. On the other hand, when the reflecting structure (or any conducting material) is placed in the near field of the antenna, there is a nonnegligible coupling due to induced currents by the antenna on these elements, and the overall electromagnetic properties of the latter change thereby. Diffraction and scattering effects from the edges of the antenna and from the reflecting structures within this near-field zone may therefore make a substantial contribution; physical optics would then provide a significantly better approximation than geometric optics in describing these effects.

The effects of near-field scattering have not been explicitly addressed in the GPS literature. On the other hand, the effects of transmitting and receiving element multipath on the code and on the phase GPS observables have been addressed at some depth in the GPS literature. *Counselman and Gourevitch* [1981] studied the effects of multipath interference and sky blockage on a method of ambiguity resolution. *Young et al.* [1985] experimented with multipath effects originating at the Block I GPS satellite antenna and derived an expression for the error on the pseudorange and carrier signal observables introduced by single multipath reflections. This effect will be the same at all identical receiving antennas for sites located close together and will therefore cancel out in difference positioning. Although we have not addressed the effect in this paper, similar efforts to assess quantitatively the impact of multipath caused by the Block II satellites on global positioning should be carried out, especially as the accuracy of geodetic measurements with GPS improves. Many tests have been performed to evaluate the

severity of signal multipath effects on the GPS pseudorange measurements [*Bletzacker*, 1985] and their impact on the accuracy of orbit determinations [*Evans and Carr*, 1989]. Many tests also have dealt with inducing such errors by means of artificial reflectors placed near the antenna to study the effect in controlled environments [e.g., *Greenspan et al.*, 1982; *Tranquilla*, 1986; *Tranquilla et al.*, 1986]. *Georgiadou and Kleusberg* [1988] discussed errors in GPS phase observables resulting from multipath interference and presented a mathematical model for multipath errors produced by multiple simultaneous reflections.

Multipath as a potential source of error on geodetic estimates of site position from GPS data has been discussed in some detail in the literature. *Davis et al.* [1989] found the effect of multipath on ~20-m baselines to be limited to ~1 mm both in repeatability and on accuracy. *Genrich and Bock* [1992] employed a method to filter out the daily repeating multipath signals to show submillimeter daily repeatability for ~100-m baselines.

In the following, we study the effects of scattering associated with the receiving antenna on estimates of geodetic site positioning with GPS. We first develop a theoretical model for carrier phase multipath effects, which follows closely the method and formalism of *Young et al.* [1985] and of *Georgiadou and Kleusberg* [1988]. In particular, we assume that the effect of multipath on the carrier phase signal is described by the reflectivity of the reflecting material and by the relative positions and orientations of the transmitting satellite, the reflecting object, and the receiving antenna. We present experimental evidence of the presence of signal scattering effects in data acquired from a pillar-mounted GPS antenna, identical to many of those used in the continuously operating International GPS Geodynamics Service (IGS) network. Although multipath is a far-field phenomenon, as we discussed earlier, the multipath error model we develop here should prove useful in assessing the scattering effects. We describe how elevation angle cutoff tests [e.g., *Davis et al.*, 1985] can be used to assess quantitatively the effect of multipath errors on site position estimates. Finally, we demonstrate that microwave absorbing material reduces the low-frequency component of the multipath effect.

Multipath-Induced Errors

In making GPS observations, we use antennas with low directive gain (designed for full hemispheric coverage) to acquire data simultaneously from as many visible satellites as the receiver will allow. "Visible" here means a direction with positive elevation angle as viewed from the receiving antennas. This design requirement means that reflected/scattered signals arriving from any positive elevation angle cannot be rejected. We would nevertheless like to be able to reject entirely all signals arriving from negative elevation angles, as well as all signals with left-hand circular polarization (LCP). As an example, Figure 1 shows the RCP and LCP antenna gain patterns for the L1 frequency of a Dorne-Margolin GPS antenna with concentric choke rings. (Brand names are mentioned for identification purposes only.) This type

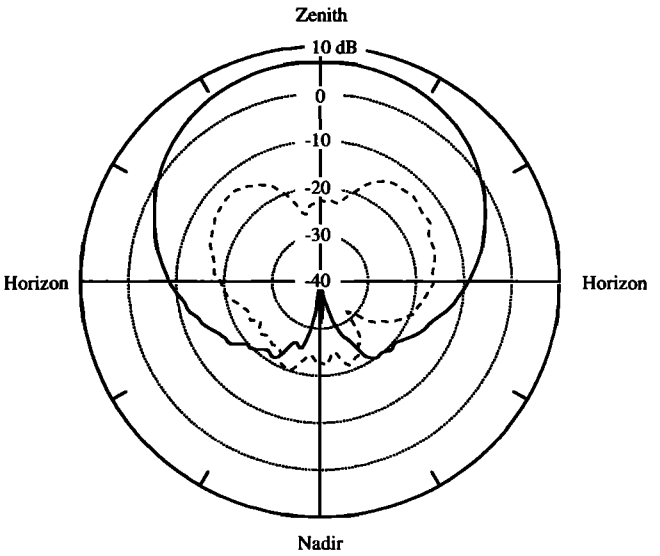

Figure 1. Cut through the main lobe axis of the right- (solid) and left-hand (dashed) circular polarization antenna gain patterns of the L1 frequency for a Dorne-Margolin Global Positioning System antenna with choke rings. The radial coordinate represents gain in decibels. The zenith point corresponds to the 0 degrees direction. The maximum (6.75 dB) and minimum (−40.55 dB) of the right-hand circular polarization gain occur at a zenith angle of 3°and 171°, respectively (M. L. Exner, personal communication, 1994).

of antenna/backplane configuration is in common use at sites in the global GPS network. The corresponding L2 antenna-gain patterns are qualitatively similar. The concentric choke rings of these antennas [e.g., *Tranquilla et al.*, 1994, and references therein] have been engineered as a compromise among gain and phase pattern characteristics, polarization isolation, and portability. The existence of nonzero antenna gain below the horizon, furthermore, represents an antenna design balance between the rejection of reflected signals and the acceptance of unreflected signals at low positive elevation angles. In Figure 1 we can see that the gain at an elevation angle of −45°, for example, is about 30 dB lower than the gain at zenith. Thus reflected signals impinging from negative elevation angles are not completely eliminated. To achieve this attenuation the antenna gain has had to be gradually reduced toward low positive elevation angles. Since the sense of circular polarization of the GPS satellite signals will change upon each specular reflection from perfectly conducting surfaces, single-reflection (or any odd number reflection) effects can be reduced by antenna polarization discrimination. However, no polarization discrimination is possible for reflected signals reaching the GPS antenna phase center after an even number of reflections. *Schupler et al.* [1994] characterized the electrical properties of several different models of GPS antennas used for geodetic measurements. All these antennas share the property that signals from negative elevation angles are not completely rejected.

To quantify the effect of multipath on estimated parameters, we must consider the method used to obtain

the estimates. Generally, a linear least squares technique is involved in GPS data analysis. The basic observables are generally the ionosphere-free linear combination (LC) of the L1 and L2 phase observables. The pseudorange observables are sometimes used as well, but they carry little weight relative to the phase observables. In most analyses, the observable used is the so-called "double differenced" LC phase [*King et al.*, 1985], in which between-satellite and between-site differences of the LC phases at each epoch are formed. The clock errors in (1) cancel upon formation of the double differences, and thus clock parameters need not appear in the solution. A different way of dealing with the clock errors is for clock parameters to appear explicitly in the analysis. With this latter technique, a stochastic filter is used to estimate the time variation of the clock parameters. A stochastic filter can also be used to estimate the atmospheric zenith delays [e.g., *Tralli and Lichten*, 1990].

The modeling of the atmospheric propagation delay in the analysis of space geodetic data has received a great deal of attention in the last few decades, mainly because of its importance in the analysis of VLBI data. Serious attempts to improve the models developed in the late 1960s and early 1970s were made by *Davis et al.* [1985] and by *Lanyi* [1984]. More recent models [e.g., *Herring*, 1992; A. E. Niell, Global mapping functions for the atmosphere delay at radio wavelengths, submitted to *Journal of Geophysical Research*, 1995 (hereinafter referred to as A.E. Niell, submitted manuscript, 1995)] are believed to be superior. The main effort was directed toward increasing the accuracy of the so-called mapping function of the hydrostatic delay for low elevation angles ($\lesssim 10°$). These studies quantified the effects of systematic errors in the mapping function at low elevation angles on estimates of the vertical coordinate of site position [*Davis et al.*, 1985]. Data from low elevation angles are useful in VLBI, as well as in GPS, to reduce the correlation between estimates of the vertical component of site position and estimates of the corresponding zenith propagation delay.

The problem of the atmospheric propagation delay in the analysis of GPS data is different from that in the analysis of VLBI data. Although the technique could in principle benefit from low-elevation angle observations, GPS data are almost always acquired above elevation angles of $\sim 15° - 20°$, due mainly to the reduced signal-to-noise ratio (SNR) which the antenna pattern imposes on observations from lower elevation angles (see Figure 1) to lessen the effects of multipath. At such relatively high elevation angles, errors in the estimates of the atmospheric propagation delay due to inadequacies in the elevation angle mapping function are usually quite small, always less than 5 mm, and less than 1 mm for nearly all cases [*Davis et al.*, 1985; *Lanyi*, 1984; *Herring*, 1992; A .E. Niell, submitted manuscript, 1995]. Horizontal gradients in the wet refractivity of air, as measured by microwave water vapor radiometers may cause azimuthal asymmetries of 30 mm or more in propagation delay at an elevation angle of 20° [*Davis et al.*, 1993]. However, systematic errors in models of the atmospheric propagation delay have not been shown to be a major source of error in GPS if stochastic corrections to the zenith propagation delay are estimated. Nevertheless, when atmospheric propagation delay parameters are estimated, the effects on site position estimates of other elevation angle-dependent systematic errors, non atmospheric in origin, can be "magnified" because of the high correlations mentioned above.

It has long been understood that multipath effects are greater for data acquired from satellites at lower elevation angle [e.g., *Bletzacker*, 1985]. Assessments of the influence of multipath on estimates of site position [e.g., *Davis et al.*, 1989] have not generally detected serious effects. The difficulty in developing a quantitative understanding of the effects of multipath has been the inherent dependence of multipath on the radio-reflective environment. Below, we study this situation using a simple model.

Effects of Multipath on GPS Phase Observables

In this section we develop a model for the effects of carrier phase multipath. This development is similar to that presented by *Young et al.* [1985] and *Georgiadou and Kleusberg* [1988]. We redevelop the model here to expose its details. Implicit in this model is the (often incorrect) assumption that the reflecting structure is located in the far field of the antenna so that geometrical (ray) optics, as opposed to physical optics, can be applied.

The model assumes that (1) the incoming GPS signal is a plane wave, and (2) there exists a single planar horizontal reflector, infinitely large, located a distance H beneath the GPS antenna phase center. (We ignore variations of the position of the phase center with signal direction [see *Schupler et al.*,1994].) Under these assumptions, the signal at the antenna phase center is the sum of two signals, the signal arriving from the direct line of sight to the satellite, and the reflected signal. Figure 2 illustrates the single-reflector multipath geometry. The signal transmitted by the GPS satellite arrives at the receiving antenna at an incident elevation angle ϵ with respect to the horizon. The orbital motion of the GPS satellite in the sky relative to the position of the antenna on the ground results in an incident elevation angle $\epsilon(t)$ which is time dependent. Thus we write the signal received at the antenna phase center, $A(t)$, as the sum of the unreflected signal, $U(t)$, and the reflected signal, $R(t)$:

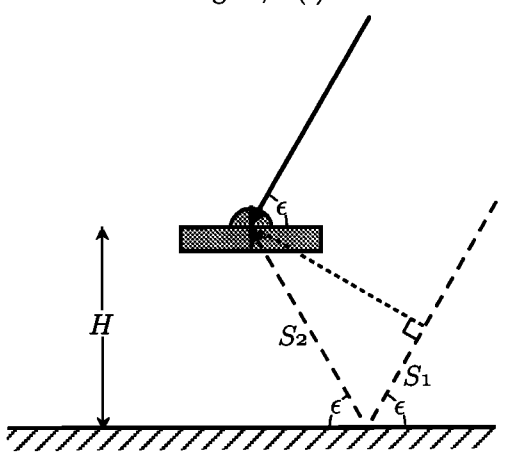

Figure 2. Diagram of the single-reflector geometry ($\epsilon \geq 45°$) for multipath model.

$$A(t) = U(t) + R(t) \tag{2}$$

where A, U, and R represent the complex electric or magnetic field of the respective signals. If we focus on the carrier signal of frequency f, then the unreflected wave may be represented by

$$U(t) = U_o e^{-2\pi\imath ft} \tag{3}$$

where U_o is complex. (The negative sign of the phase is arbitrary and is determined by the way in which the phase is defined. *Leick* [1990], e.g., defines the phase negative to that of (1). For a definition of the form of (1), the negative sign in (3) is appropriate.) The reflected and unreflected signals have the same source, but to reach the phase center the reflected signal must travel an additional distance $S_1 + S_2$ (see Figure 2). The signal is attenuated through reflection and the antenna power pattern by an amount α ($0 \le \alpha \le 1$) assumed real:

$$R(t) = \alpha U(t - \frac{1}{c}[S_1 + S_2]) \tag{4}$$

where c is the speed of light. (We ignore the extra atmospheric propagation delay due to the reflected path, which is equivalent to $\lesssim 3$ μm, and phase and polarization changes which might occur on reflection. Also, for elevation angles $\epsilon < 45°$, the geometry of Figure 2 changes, but the result given below is unchanged.) Combining (2)–(4), we obtain

$$A(t) = U_o e^{-2\pi\imath ft}\left(1 + \alpha e^{2\pi\imath\frac{S_1+S_2}{\lambda}}\right) \tag{5}$$

where $\lambda = c/f$ is the wavelength.

From Figure 2 we find

$$\begin{aligned} S_1 &= -S_2 \cos 2\epsilon \\ S_2 &= H \csc\epsilon \end{aligned} \tag{6}$$

The received signal $A(t)$ can also be written in terms of the unreflected signal $U(t)$ and a change in its amplitude by a factor β and its phase by $\delta\phi$ as

$$A(t) = \beta U(t) e^{i\delta\phi} \tag{7}$$

In (7), β and $\delta\phi$ are implicitly time dependent.

Comparing (3), (5), (6), and (7), we can express the multipath contribution $\delta\phi(\epsilon;\alpha,H,\lambda)$ to the phase as

$$\delta\phi(\epsilon;\alpha,H,\lambda) = \tan^{-1}\frac{\alpha\sin\left[4\pi\frac{H}{\lambda}\sin\epsilon\right]}{1+\alpha\cos\left[4\pi\frac{H}{\lambda}\sin\epsilon\right]} \tag{8}$$

The multipath contribution, under the assumptions made above, thus depends on four parameters: the vertical distance, H, from the reflector horizontal plane to the antenna phase center; the attenuation, α, of the voltage amplitude of the reflected signal; the observing wavelength, λ; and the elevation angle, ϵ, of the incident signal.

Before examining the effects of multipath on estimates of site position, we present several useful expressions. It is standard in GPS studies to speak of phase, not in radians, as in (8), or in cycles, as in (1), but in units of length.

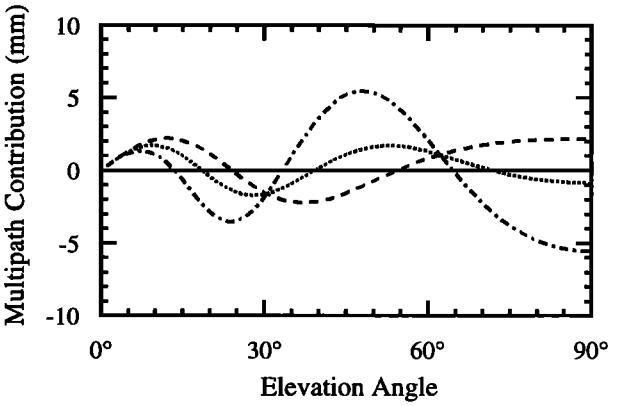

Figure 3. Multipath contributions for the L1 (dotted), L2 (dashed), and linear combination (dot-dashed) phase observables, in units of length as per (9), based on the multipath model (8) and (10). The calculations used H = 150 mm and $\alpha = 0.06$.

The contribution of multipath to the phase, expressed in these latter units, which we denote with a subscript L, is thus

$$\delta\phi_L(\epsilon;\alpha,H,\lambda) = \frac{\lambda}{2\pi}\delta\phi(\epsilon;\alpha,H,\lambda) \tag{9}$$

As discussed above, most GPS analyses make use not of the carrier phase observables themselves but of the ionosphere-free linear combination (LC). Expressed in units of length, the LC multipath phase contribution for the L1 and L2 frequencies is

$$\begin{aligned} \delta\phi_L^{\mathrm{LC}}(\epsilon;\alpha,H) \simeq\ & 2.5457 \times \delta\phi_L(\epsilon;\alpha,H,\lambda_1) - \\ & 1.5457 \times \delta\phi_L(\epsilon;\alpha,H,\lambda_2) \end{aligned} \tag{10}$$

where λ_1 is the L1 wavelength (0.19029 m) and λ_2 the L2 wavelength (0.24421 m). The two constants in (10) are derived from the values for λ_1 and λ_2 [*Spilker*, 1978]. Figure 3 shows the multipath contribution to the L1, L2, and LC phases for H = 150 mm and α = 0.06. (The reason for these choices will be explained later.) The LC multipath contribution as a function of elevation exhibits a "beating" of the L1 and L2 multipath contributions. Constructive "interference" occurs when the multipath contributions effects on the L1 and L2 phases are of different sign; destructive "interference" occurs when the L1 and L2 multipath contributions are of the same sign.

This "interference" is more clearly seen in Figure 4, which shows the effect on the LC phase of multipath from (10) for three different choices of H: 0.15 m, 0.60 m, and 1.00 m. The attenuation α is 0.06 in all three cases. When plotted as a function of elevation angle, the effect of multipath appears sinusoidal. For $\alpha \ll 1$ the maximum amplitude is proportional to α and the elevation "wavelength" is proportional to λ/H. Antennas are generally placed 1 m or higher above the ground for tripods and for most pillar mounts. It is usually also possible to set up the antennas at least several meters from other multipath sources (walls, fences, etc.). One might therefore surmise that there is a greater chance for multipath effects to "cancel out" when averaged over a range of observed elevation angles for larger values of H. Below, we perform

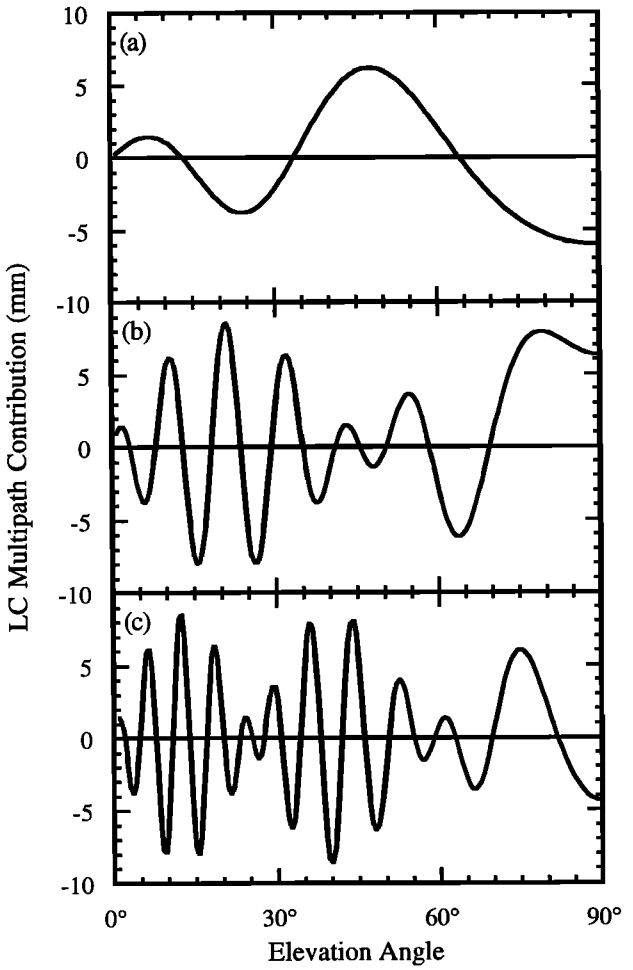

Figure 4. Multipath contributions to the linear combination (LC) phase observable for $\alpha = 0.06$ and for three values of the parameter H: (a) $H = 0.15$ m; (b) $H = 0.6$ m; and (c) $H = 1$ m.

a quantitative assessment of the effects of multipath on GPS estimates of site position.

Effects of Multipath on GPS Estimates of Vertical Coordinate of Site Position

We used a simplified analysis to determine the effects of multipath. First, we limited our study to least squares inversions, which are easier to understand in detail than are stochastic filters. We also concentrated on the errors in the estimated vertical coordinate of site position, since, from our discussion above, we knew it to be highly influenced by elevation angle-dependent errors. Further, we did not consider errors in the estimates of satellite orbit parameters. Our model for the effects $\delta\phi_L(\epsilon)$ of multipath on GPS observations contained three parameters: (1) an ambiguity constant δC_o, (2) an atmospheric zenith propagation delay $\delta\tau_a^z$, and (3) an adjustment δz to the vertical coordinate of site position:

$$\delta\phi_L(\epsilon) = \delta C_o + \delta\tau_a^z \csc\epsilon + \delta z \sin\epsilon \qquad (11)$$

Effects of multipath on estimates of horizontal position are considered below. When the effects of multipath on the LC phase from (10) are used in the left side of (11), then the estimates of the parameters in (11) determined by least squares inversion represent the errors in those parameters caused by multipath.

For the observations, we chose a realistic distribution of elevation angles and then carried out the least squares inversion. Figure 5 shows this distribution in a polar coordinate plot; it corresponds to January 15, 1994, for the Westford GPS site (latitude N 42°61, longitude W 71°49), and a minimum elevation angle of 5°.

We found that the errors in the estimated parameters strongly depend on the minimum elevation angle of the data used in the solution, the so-called "elevation angle cutoff." We performed elevation angle cutoff tests with and without a zenith delay parameter being estimated. Figure 6 shows the errors in the estimated vertical coordinate of site position as a function of minimum elevation angle for the values of H and the value of α used for Figure 4. These "cutoff tests" demonstrate that (1) the error in the estimate of the vertical coordinate of site position can become dramatically large for reflective objects placed close to the antenna phase center and for high cutoff angles, and (2) this error becomes "magnified" when a correction to the zenith atmosphere propagation delay is estimated simultaneously. The implications for accurate determination of vertical position are clear: a small (5° to 10°) change in the elevation minimum can change the estimates of the vertical coordinate of site position by tens to hundreds of millimeters. Since typical standard errors for determinations of the vertical coordinate of site position are believed to be ~5 mm, these results indicate that multipath may be a significant source of error.

We have considered how the error in the estimate of the vertical varies when the cutoff angle only is changed. Under the assumptions of our multipath model and simplified analysis, if the cutoff angle were to remain fixed

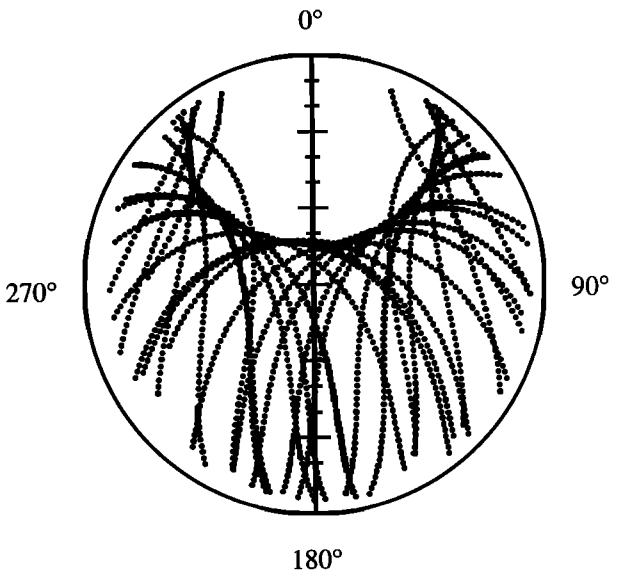

Figure 5. Global Positioning System satellite position plot for the Westford site (latitude N 42°61, longitude W 71°49) for a 24-hour period. The zenith point ($\epsilon = 90°$) corresponds to the center of the plot, the horizon ($\epsilon = 0°$) to the outer circle.

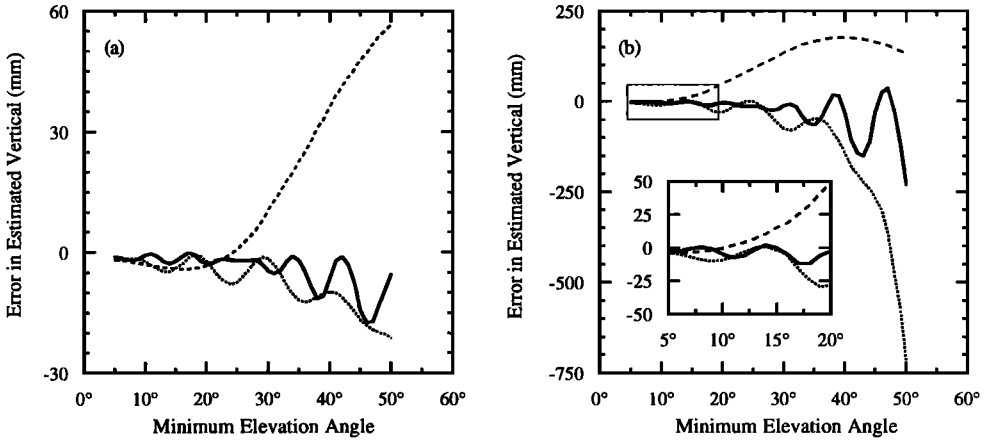

Figure 6. Estimate of the vertical coordinate of site position as a function of minimum elevation angle, relative to the estimate for a 5° minimum elevation angle ("elevation angle cutoff test") for the multipath phase error model and the elevation-azimuth distribution of Figure 5, (a) without and (b) with simultaneous estimate of zenith atmospheric propagation delay. The calculations used $\alpha = 0.06$ and three values of the parameter H: $H = 0.15$ m (dashed); $H = 0.6$ m (dotted); and $H = 1$ m (solid).

over time, then the error in the vertical position estimate would also remain fixed over time. The error would thus not affect determinations of site velocity, which are important in a wide variety of crustal deformation studies. Unfortunately, it is not possible to exercise such a degree of control over GPS data acquisition. For example, with the recent onset of Anti-Spoofing (AS) for all the Block II spacecraft, acquisition of the precise code signals are no longer possible. Some receivers have therefore switched to a cross-correlation mode, which in effect decreases the SNR of the phase measurements. To counter this problem, analysts have begun using an elevation cutoff angle of 20°, whereas before AS a cutoff angle of 15° was typically used. Of course, not only the minimum elevation angle, but any change in the elevation coverage used in the solutions will cause changes in the errors of the parameter estimates. Such a change would occur, for example, if a satellite were to become disfunctional or if estimates were obtained from observations made during different blocks of sidereal time (the GPS constellation provides a nonuniform elevation angle distribution of the visible satellites in the observer's sky).

Systematic Errors in Estimates of Baseline Components

In this section we present experimental evidence of the presence of errors due to signal scattering on estimates of baseline components in data acquired at one site of the permanently operating GPS network. This site (antenna-receiver system and antenna monumentation) is identical to at least 11 other sites in the continuously operating GPS Global Tracking Network for the IGS (S. DiNardo, JPL, private communication, 1994).

In early 1993, NASA and the National Oceanic and Atmospheric Administration (NOAA) started operating a temporary GPS receiver at Westford (monument WES2), Massachusetts, for the IGS and Fiducial Laboratories for an International Natural Science Network (FLINN). In January 1994 a permanent GPS site was selected at Westford, and its monument erected (monument WFRD). The WFRD antenna is centered over a permanent monument by means of a supporting ring, a spike, and three leveling feet. The monument is an ~1-m-high concrete column, 0.75 m in diameter, with a metallic plate 0.45 m in diameter centered on and laid flush with the top of the concrete. The vertical distance from the top of the concrete to the antenna phase center is 0.20 m (Figure 7).

To investigate the radio reflective environment of the pillar-mounted antenna, a tripod-mounted antenna was set up over another mark, WFR2, a horizontal distance of only ~2.2 m from the WFRD mark. The WFRD and WFR2 GPS systems both consisted of TurboRogue SNR-8000 receivers and Dorne-Margolin antenna-plus-choke ring assemblies. The observations consisted of samples of undifferenced dual-frequency carrier phase and pseudorange measurements obtained every 30 s from 6 to 8 satellites. We used a standard strategy to process the GPS data using the GPS Inferred Positioning System (GIPSY) software [*Webb and Zumberge*, 1993, and references therein]. Using the data from each day (starting at 0 UTC), we formed the carrier phase and pseudorange ionosphere-free linear combination and estimated the three components of position of WFRD relative to WFR2, carrier phase ambiguities, and satellite and station clocks. No tropospheric zenith delays were estimated. Precise orbits and consistent Earth rotation parameters were procured from IGS and were not further estimated in the analysis. For a baseline of this length, the ionospheric effects are negligible and use of the ionosphere-free linear combination increases the noise about threefold and twofold relative to the L1 and L2 observables, respectively. Our choice of the "noisier" LC was motivated by the general use of this observable for analyzing data for longer baselines. All ambiguities were successfully resolved and subsequently fixed to integer values.

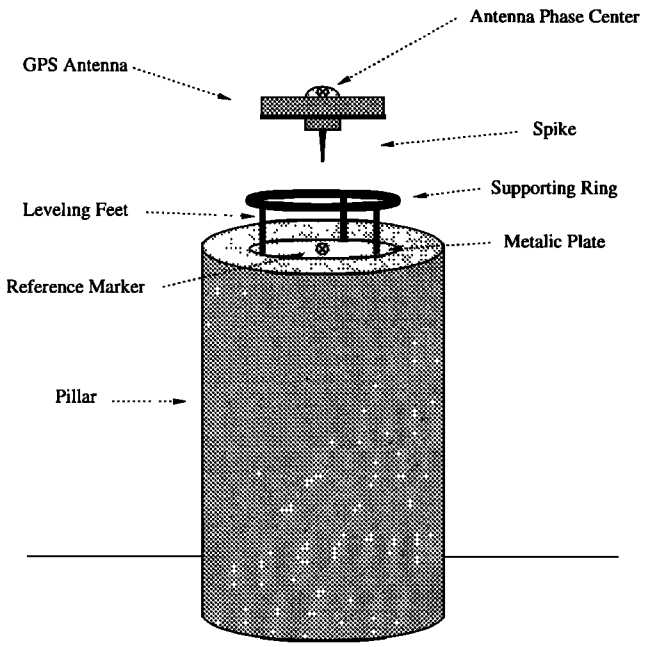

Figure 7. Sketch of the WFRD permanent Global Positioning System (GPS) antenna and monument, located at Westford, Massachussets. (Drawn to scale. For reference, the diameter of the antenna is 0.381 m.)

The root-mean-square (rms) postfit LC phase residual was typically ~3 mm, and no systematic patterns were apparent in the phase residuals plotted as a function of time (Figure 8a). When plotted as a function of elevation angle, however, the postfit LC phase residuals displayed a clear systematic dependence (Figure 8b). No azimuth dependence was apparent (Figure 8c), other than that associated with the elevation angle dependence. The fact that no signature could be seen when the residuals from all the satellites to a site were plotted versus time or versus azimuth angle indicated that the error was mainly elevation angle dependent. Since the 6–8 satellites visible simultaneously represented a range of elevation angles, the systematic behavior was not visible in a time or azimuth plot involving all the satellites. The systematic behavior was visible in the residuals for any given individual satellite when displayed as a function of elevation angle, time, or azimuth (Figure 9).

To investigate the possibility that the residuals were caused by a software error, we processed some of the data sets with the Bernese software version 3.4 [*Rothacher et al.*, 1993, and references therein]. This software explicitly uses double-differenced data, and hence no clocks are estimated in the solutions. Otherwise, there should be no difference between the estimates obtained from the two analysis packages. (GIPSY uses a stochastic filter to estimate the time dependence of the zenith atmospheric propagation delay, whereas the Bernese software estimates constant values for a given time interval; since we were not estimating these parameters, this difference should not affect the comparison.) The results obtained with the GIPSY and the Bernese software for the baselines investigated were fully consistent. (For the April 17 data set discussed above, the nine values of the elevation angle cutoff test determined using the two analysis packages had an rms difference of 0.3 mm.)

The systematic trend in the residuals repeated itself in all the data sets we obtained over an 8-day period. (In fact, this trend has been seen since WFRD was installed.) Figure 10 shows an example of the postfit LC phase residuals that involve GPS satellite 22 (i.e., PRN 22), observed on April 9 and 10, 1994. The qualitative similarity between the two curves is confirmed quantitatively in Figure 11. The (day-to-day) cross-correlation coefficient function for the time series shown in Figure 10 peaks at a value of 0.70 at a delay time of 4 min. For an error that depends solely on satellite position, the cross-correlation peak should occur 3.93 min later on each successive day since the satellite constellation repeats itself once per sidereal day. The data of Figure 10 were recorded, as described above, every 30 seconds, which is therefore the resolution of the curve in Figure 11. The repeating signature can therefore effectively be removed by

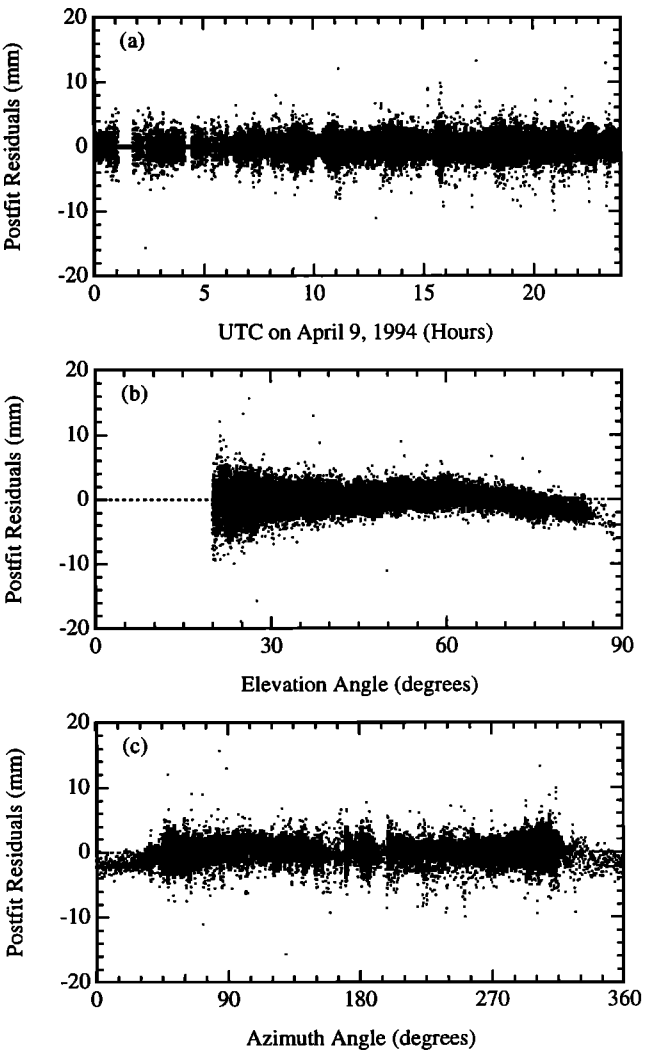

Figure 8. Postfit linear combination phase residuals for the 2.2-m WFRD-WFR2 baseline, plotted as a function of (a) time, (b) elevation angle, and (c) azimuth. Data were acquired every 30 s for 24 hours on April 9, 1994.

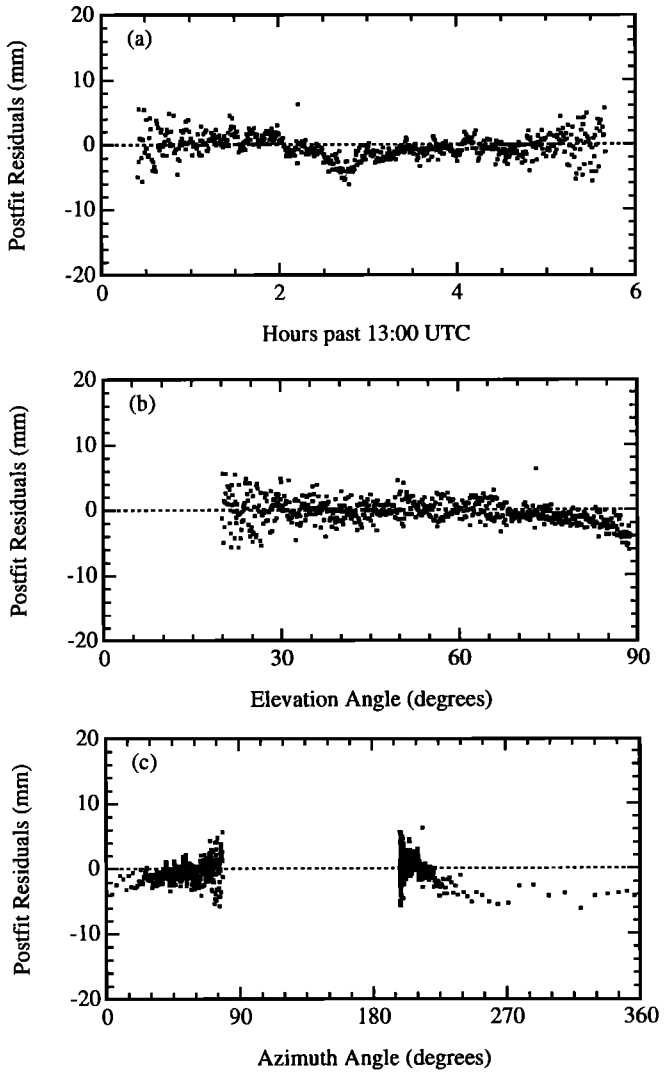

Figure 9. Same as Figure 8, except data from the satellite PRN 22 are shown.

differencing the residuals, adjusting for the daily ~4-min advance. The rms scatter of the differences for the residuals of Figure 10 is 1.8 mm, whereas if the two data sets were independent, the rms scatter of the difference should be the root-sum-square of the rms residual for PRN 22 from each of the two days, or 2.7 mm. The high degree of day-to-day correlation demonstrates that the error causing the systematic behavior is associated with repeated satellite-to-antenna geometry. Two sources of error that meet this criterion are signal reflections/multipath and antenna phase-center variations.

Antenna phase-center variations, as they are commonly understood, are due to the nonsphericity of the antenna phase pattern and therefore are independent of the antenna environment. (In fact, one may think of multipath or scattering as a modification of the antenna phase pattern.) *Schupler et al.* [1994] used an anechoic chamber to measure the L1 and L2 phase pattern, phase center location, amplitude pattern, and axial ratio pattern of several different models of GPS antennas used for geodetic measurements and demonstrated that each of the antennas

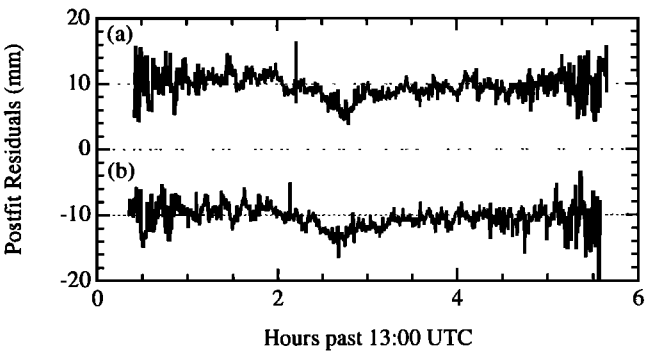

Figure 10. Postfit linear combination phase residuals for the 2.2-m WFRD-WFR2 baseline from PRN 22 for ~5 hours on each of two consecutive days: (a) April 9, 1994, and (b) April 10, 1994. The two series of residuals have been offset (by +10 and −10 mm) for clarity.

displays anisotropic phase center variations at the centimeter level (a few tens of degrees of phase at L-band). For the type of antenna used in the experiments presented in this paper, the Dorne-Margolin antenna with choke ring, the phase pattern is nearly isotropic, with rms azimuthal variations at the 1–2 mm level; by contrast, phase center variations amount to ~10–14 mm, peak-to-peak, over an elevation range of 0°–90°. If the phase pattern is similar for all antennas of the same make and model (microstrip patch antennas, like Dorne-Margolin, are manufactured with very repeatable techniques, and *Schupler et al.* [1994] concluded that variations between such antennas are insignificant for geodetic purposes), then for this short-baseline experiment we would not be sensitive to phase center variations because the difference in elevation angles from the ends of a ~2.2-m baseline for a given satellite at a given epoch is negligible. To investigate the possibility that the antenna phase patterns are different, we switched the GPS antennas (but not the receivers) of the WFRD and WFR2 sites. The WFR2 antenna was mounted on a standard surveying tripod. With the antennas switched, we again obtained and processed the data from this baseline. If the source of the error were

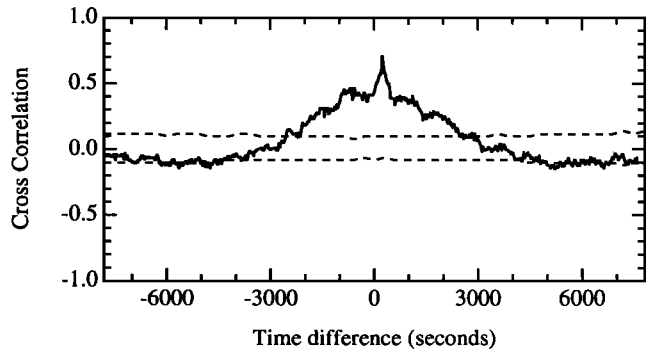

Figure 11. Cross correlation for the two time series shown in Figure 10. The cross correlation is a maximum for $\tau = 240$ s, with a peak value of 0.70. The dashed lines indicate the range between which the cross correlation should fall 99% of the time, under the hypothesis that the data from the two days are uncorrelated.

antenna-dependent, then the error should change signs when the antennas were switched. The results, however, were unchanged. We also tried switching receivers, and the results were again unchanged. The results of these tests led us to believe that the effect was caused by the environment specific to the WFRD antenna. We tentatively concluded that the effect was caused by scattering and reflections from the WFRD pillar-antenna combination, since data obtained from the WFR2 site, only 2.2 m away, did not seem to suffer from these effects. Additional support to this conclusion came from analysis of the WES2-WFRD and WES2-WFR2 baselines. (WES2 is located ~580 m to the northeast of both WFRD and WFR2 and consists of the same type of antenna-receiver system.) We processed the data from these two baselines independently; the elevation angle-dependent error was associated with WFRD. Examination of data from three other tripod-mounted antennas temporarily set up over reference marks in the surroundings of WFRD (at distances of approximately 613, 1066, and 1698 m from the latter) also supported our conclusion.

To further quantify the elevation angle-dependent error, we performed cutoff angle tests. Using our study described above, we should be able to relate the results of the cutoff angle test to parameters in the multipath model (H and α) under our hypothesis of reflections from the surface of the pillar. Figure 12 contains the results from the cutoff angle tests. For this short-baseline test, no zenith atmospheric propagation delay parameters were estimated. Plotted are the values, relative to those for the 5° cutoff angle solution, of the estimates of the north, east, and vertical components of the ~2.2-m WFRD–WFR2 baseline, as a function of minimum elevation angle. The error bars are the statistical standard deviations of the differences [*Davis et al.*, 1985], based on our adopted standard deviations of 3 mm for the LC phases, typical values for the rms postfit LC phase residuals (see above). The cutoff angle test results of Figure 12 display significant centimeter-level systematic deviations from zero for the estimates of the vertical component; the results for the horizontal components show insignificant deviations from zero.

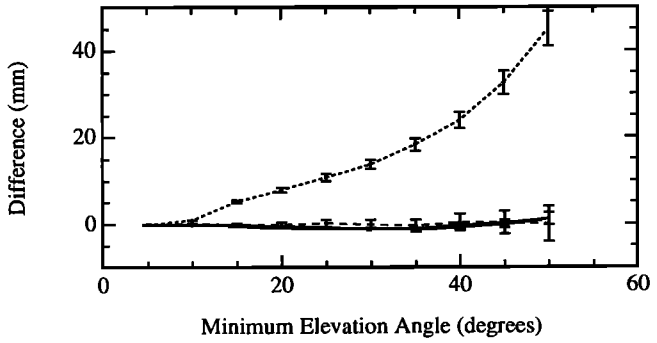

Figure 12. Example of elevation angle cutoff test for the WFRD-WFR2 data obtained on April 17, 1994 (see text). Results are shown for the three local geodetic components of position of the WFRD antenna: north (solid), east (dashed), and up (dotted). The position of the WFR2 antenna was held fixed, and no zenith atmospheric propagation delay parameters were estimated. The error bars are the statistical standard deviations of the differences (see text) between the indicated solutions and the 5° solution.

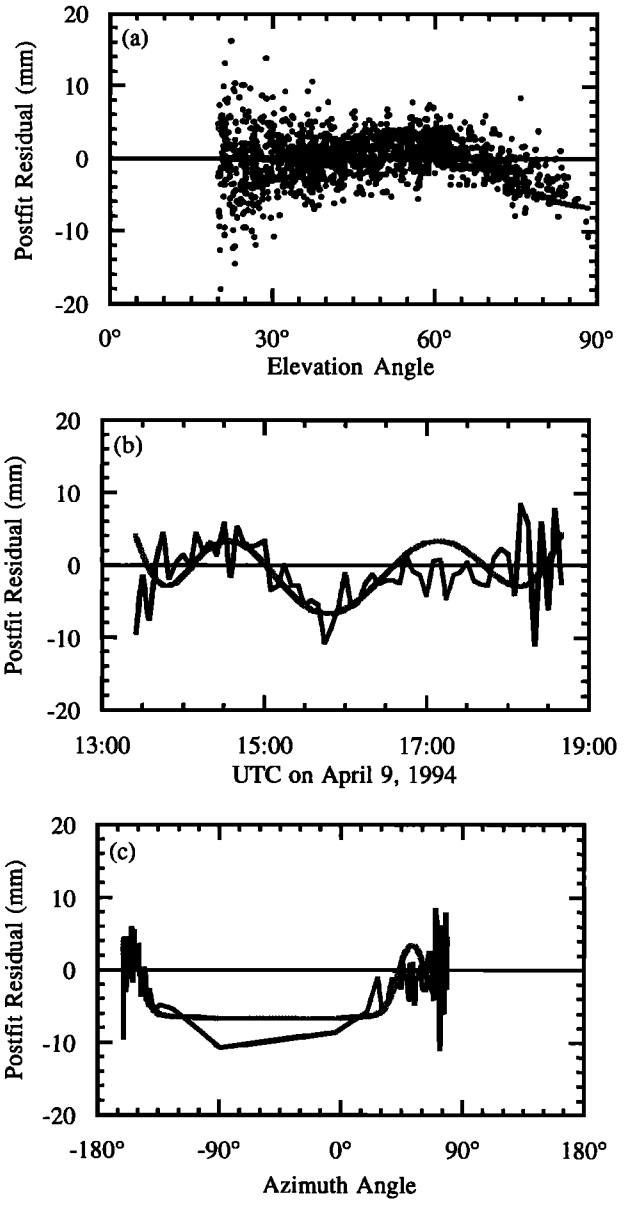

Figure 13. (a) Postfit linear combination phase residuals for the WFRD-WFR2 baseline for all satellites from the April 9, 1994, data, plotted as a function of elevation angle. The gray line shows the simulated residuals based on the simple multipath model with values of $H = 130$ mm and $\alpha = 0.01$. (b) Same as Figure 13a, except that residuals for only satellite PRN 22 are shown, only every tenth data point is shown, and the residuals are plotted as a function of time. (c) Same as Figure 13b, except the residuals are plotted as a function of azimuth.

The results of the cutoff angle tests show qualitative similarities to those determined from the simulations for values of H and α in the ranges 100–200 mm and 0.05-0.10, respectively. The simulations, however, fail to reproduce the results of the cutoff angle tests for minimum elevation angles $\lesssim 20°$; the inflection in the estimate of the vertical component at about 20° seen in Figure 6a is not

present in Figure 12, probably due to the inadequacy of our simple multipath model.

As a further test of our multipath model, we used our simulation approach to calculate values of postfit LC phase residuals. Although this check is not completely independent, since the data used to generate the results from the cutoff angle test and the postfit LC phase residuals are the same, neither is it completely redundant, for no one-to-one relation exists between the postfit residuals and the results of the cutoff angle test. In Figure 13 we present the postfit residuals from this simulation for $H = 130$ mm and $\alpha = 0.1$ along with the observed postfit LC phase residuals. We also present a typical comparison in Figure 13 for a single satellite. The model reproduces the several-hour timescale behavior quite well but fails to account for the higher-frequency variations.

In deriving the multipath model of the previous section, we assumed that ray (geometric) optics could be used. Such an assumption is valid when the reflecting structure is located in the far field of the antenna. The boundary between the near-field or Fresnel zone and the far-field or Fraunhofer zone of an antenna can be determined using the expression [*Kraus*, 1988]

$$R = \frac{2D^2}{\lambda} \tag{12}$$

where R is the distance from the antenna phase center to the boundary, D is the maximum dimension of the antenna, and λ is the observing wavelength. For the Dorne-Margolin antenna with choke ring groundplane ($D = 381$ mm; LC equivalent-$\lambda = 107$ mm) $R = 2.7$ m. Because the vertical distance from the top surface of the WFRD pillar to the antenna phase center is only ~0.2 m, the reflecting structure is located well within the near field of the antenna. Thus diffraction and scattering effects from the edges of the pillar and antenna should be significant contributors, and therefore the problem should be regarded as one of physical optics. Nevertheless, the multipath model, based on geometrical optics, appears to provide a useful approximation.

Based on the qualitative and quantitative similarities between the results from the cutoff tests for the WFRD-WFR2 data and from the simulation, and on the similarities between the postfit residuals obtained from the WFRD-WFR2 analyses and from the simulation, we hypothesized that the source of the elevation angle-dependent error is scattering from the antenna and pillar surfaces and reflection from the top of the pillar. In the next section we describe an experiment that tested this hypothesis.

Use of Microwave Absorbing Material for Reducing Scattering Effects

Modeling accurately the error due to scattering within the actual antenna environment is not easy, since a model based on ray optics is insufficient. Instead of modeling, we therefore tried to establish the main cause of the scattering via a controlled experiment. We processed LC measurements from the WFRD-WFR2 baseline with data acquired in each of two different configurations: with and without microwave absorber material placed on top of the WFRD pillar. The microwave absorber material and covered the pillar and the steel plate embedded in it and was below the choke rings attached to the Dorne-Margolin antenna of the WFRD TurboRogue (Figure 14). (We used Eccosorb HR-2 of a thickness of 5 cm and a reflectivity at 1.2 and 1.5 GHz of less than −16 dB.) Figure 15 shows the postfit LC phase residuals versus elevation angle of WFRD from the ~2.2-m baseline as obtained on two different days, one with and one without microwave absorbing material being on the pillar. The postfit LC phase residuals display a systematic dependence on elevation angle in Figure 15a (without absorber); this dependence is not evident in Figure 15b (with absorber). Figure 16 shows the difference in the rms postfit LC phase residuals of Figure 15 as a function of elevation angle. The rms residuals are reduced, in a root-difference-square sense, by about 2 mm at elevations $\gtrsim 75°$, and by about 1 mm for elevations $\gtrsim 40°$. Figure 17 shows the results from the cutoff angle tests performed using each of these two data sets. As expected based on the residuals, the systematic deviations from zero of the estimates of the vertical

Figure 14. Photograph of the WFRD permanent Global Positioning System antenna and concrete monument (foreground) with the microwave absorber in place, and the WFR2 antenna on the wooden tripod (background).

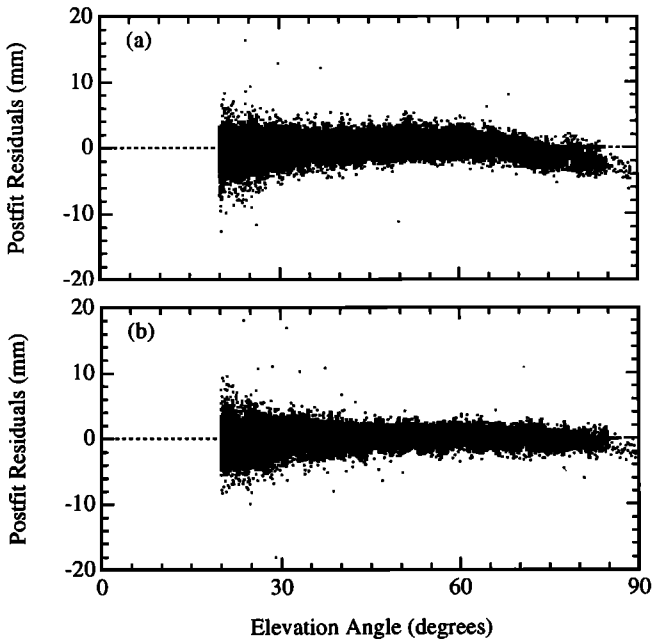

Figure 15. Comparison of postfit linear combination phase residuals for the WFRD-WFR2 baseline acquired (a) when no microwave absorber was used, on April 17, 1994; and (b) when the microwave absorber shown in Figure 14 was in place, on June 11, 1994.

component, present when the monument is not covered with absorber material, are significantly reduced (but not eliminated) when absorber material is employed.

Four other geometrical shapes and configurations of microwave absorber material were tested: (1) two layers of absorber instead of one; (2) absorber extended well over the diameter of the pillar instead of tailored to it; (3) absorber covering only the steel plate embedded in the pillar and not the concrete pillar itself; and (4) "reverse" of configuration 3. These all proved to be comparably effective at reducing the long-period (low frequency) scattering, but the first two configurations are somewhat more effective than the last two.

Effects on Estimates of Horizontal Coordinates

The results of the elevation angle cutoff test of Figure 12 indicated that the estimates of the horizontal coordinates of site position are not significantly affected by the scattering and reflection of GPS signals. To test this result, we performed simulations as before except that our observation model (11) was modified to include parameters for the horizontal coordinates. For the distribution of observations used in the previous simulations, the new simulations indicated that the predicted changes in the estimates of the horizontal coordinates were less than 0.4 mm for the north component and less than 0.2 mm for the east component. This result can be understood qualitatively by examining Figure 5, which showed that over the 24-hour observing period, the satellites rise and set over a wide range of azimuths. If the lines of sight over a particular range of azimuths were blocked, then the errors in the horizontal coordinates might not be so small. However, we have not tested this hypothesis.

Conclusions and Discussion

We used a simple model employing ray optics to study the effects of carrier phase multipath on estimates of site positions. This model depends on four quantities: the vertical distance from a horizontal reflecting surface to the antenna phase center, an average attenuation factor for all reflected signals, the observing wavelength, and the elevation angle of the incident signal. This model shows that the estimate of the vertical coordinate depends strongly on the minimum elevation angle of the data used in the analysis. The error in this estimate can become dramatically large for conducting objects placed close to the antenna phase center, due to its low-frequency nature at small ($\lesssim$0.2 m) heights, and for high-elevation angles. The error in the estimate of the vertical coordinate is further amplified when atmospheric propagation delays at zenith are estimated simultaneously with site position.

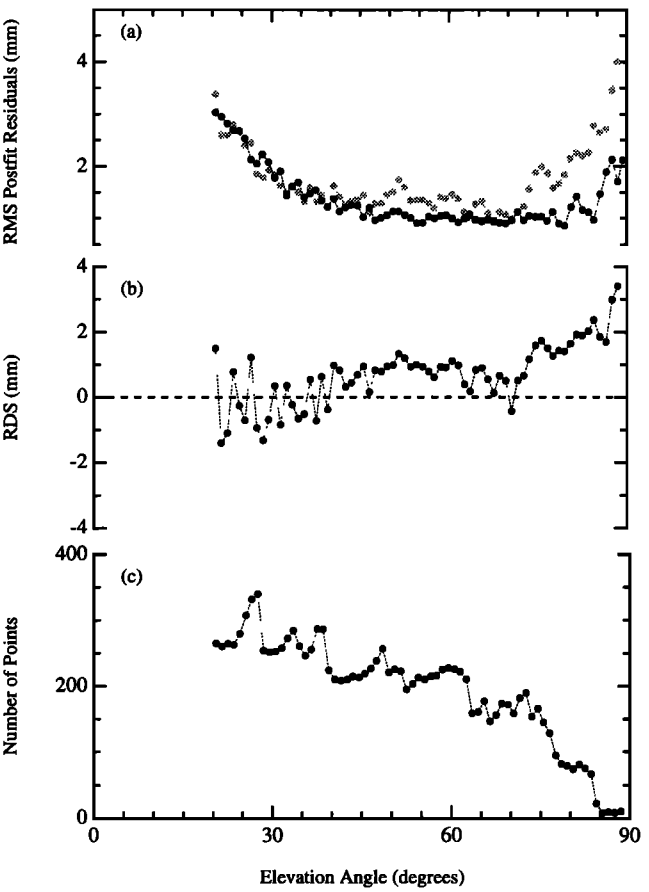

Figure 16. (a) Root-mean-square (rms) values of the postfit linear combination phase residuals for the WFRD-WFR2 baseline binned in elevation angle (bin width of 1°) for the data shown in Figure 15: April 17, 1994, no microwave absorber (gray); June 11, 1994, microwave absorber in place (black). (b) The root-difference-squared (RDS) of the rms values of Figure 16a. The RDS for each bin is defined as $\mathrm{RDS} = \mathrm{sign}(\mathrm{rms}_{\mathrm{no\,abs}} - \mathrm{rms}_{\mathrm{abs}})\sqrt{\mathrm{rms}^2_{\mathrm{no\,abs}} - \mathrm{rms}^2_{\mathrm{abs}}}$, where $\mathrm{rms}_{\mathrm{no\,abs}}$ and $\mathrm{rms}_{\mathrm{abs}}$ are the rms values for the appropriate bin, shown in Figure 16a. (c) The number of data points used to estimate values in Figures 16a and 16b.

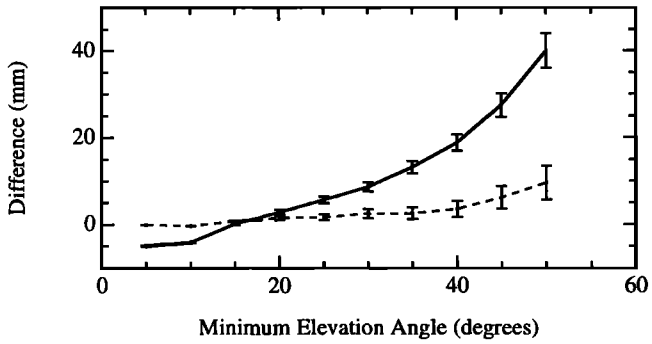

Figure 17. Difference in estimates of the vertical coordinate of site position at WFRD from elevation angle cutoff tests for the data shown in Figure 15: April 17, 1994, no microwave absorber (solid); June 11, 1994, microwave absorber in place (dashed); the ordinate origin is defined by the estimate for a 5° elevation angle cutoff with the microwave absorber in place. The error bars are as explained in Figure 12.

We found that the postfit LC phase residuals for a pillar-mounted permanent GPS antenna at Westford, Massachusetts, displayed a systematic dependence on elevation angle. The occurrence of the maximum of the day-to-day cross correlation of these residuals at a time delay of approximately 4 min demonstrated that the error causing the systematic trend was associated with the satellite-antenna geometry. The results from the elevation angle cutoff tests performed on these data displayed significant, centimeter-level changes in the estimates of the vertical component, and insignificant changes for the horizontal components, of site position. Simulations based on values for the parameters of the multipath model, $H = 130$ mm and $\alpha = 0.1$, reproduce well the long timescale behavior of the observed postfit LC phase residuals. To test the hypothesis that the source of the elevation angle-dependent effect was scattering from the top of the pillar, we placed microwave absorber material between the antenna choke ring and the pillar. The postfit LC phase residuals and the results from elevation angle cutoff tests for data collected from both ends of a ~2.2-m-long baseline with the microwave absorber in place verified the hypothesis and demonstrated the ability to reduce, by about 75%, the error in the estimate of the vertical coordinate of site position.

The results of this paper are relevant primarily to permanently mounted GPS receivers. These are usually mounted on substantial monuments, such as pillars, for stability. Unfortunately, our studies have shown that the pillar itself cannot be neglected when considering the electromagnetic environment of the GPS antenna. (The pillar is electromagnetically coupled to the antenna and is in effect part of the antenna.) The pillar surfaces scatter and its edges diffract the GPS signals. We have shown this phenomenon to be a significant source of error in the estimation of the vertical coordinate of site position. The multipath model we presented here, even though it is not appropriate for near-field problems, demonstrates that close-by reflections are a particular problem in this respect.

We have seen evidence for this error in data from the Swedish permanent GPS array, which we are using to measure three-dimensional deformation associated with glacial isostatic adjustment. There is also some evidence that scattering associated with snow which has accumulated on antenna surfaces may be an important source of error. We are currently studying these problems, which will be reported in a future paper.

The use of microwave absorbing material reduces, but does not eliminate, the error due to scattering. Another method for reducing this error would be to decrease the gain of the antenna for negative elevation angles. Increasing the diameter of the antenna and the number of choke rings would alter the gain in this way, but the effect on the gain pattern at elevation angles of interest is not clear. We are therefore performing numerical calculations based on Moment Methods [*Harrington*, 1968] to model the gain and the phase of the antenna-pillar system for various modified antenna designs. Antennas of other designs and manufacture will be included as well. The results of these studies will also appear in a future paper.

The error due to scattering in permanent GPS systems will obviously be a problem for those attempting to achieve millimeter-level accuracy in determinations of the vertical using such systems. However, all geodetic GPS studies are affected, since the data from the permanent GPS global tracking network are used to determine the satellite ephemerides which are used in geodetic analyses.

Acknowledgments. We would like to thank R. King, C. Rocken, and B. Schupler for their comments and suggestions. We would also like to thank M. Chin of NOAA for allowing us to perform tests with the Westford (WFRD) GPS antenna and for providing an additional GPS system. M. Poirier assisted in the installation and operation of the GPS systems. E. Tong, R. Blundell, and C. Papa participated in useful discussions and provided microwave absorber material for initial tests. M. Exner of the GPS/MET program at UCAR provided the data of Figure 1. P. Raffin assisted in producing Figure 14. We wish to thank P.-S. Kildal for useful discussions about the electrical properties of microwave antennas. We gratefully acknowledge use of the facilities at Westford of the Submillimeter Array of the Smithsonian Institution, which were made available to us. This work was supported by NASA grants NAG5-538 and NAS5-32353, NSF grants EAR-9105502 and INT-9214090, and the Smithsonian Institution.

References

Bletzacker, F.R., Reduction of multipath contamination in a geodetic GPS receiver, in *Proceedings of the First Symposium on Precise Positioning With the Global Positioning System*, pp. 413–422, National Oceanic and Atmospheric Administration, Rockville, Maryland, 1985.

Blewitt, G., Advances in Global Positioning System technology for geodynamics investigations: 1978-1992, in *Contributions of Space Geodesy to Geodynamics: Technology*, Geodyn. Ser., vol. 25, edited by D.E. Smith and D.L. Turcotte, pp. 195–213, AGU, Washington, D. C., 1993.

Counselman III, C.C., and S.A. Gourevitch, Miniature interferometer terminals for Earth surveying: Ambiguity and multipath with Global Positioning System, *IEEE Trans. Geosci. Remote Sens.*, *GE-19*, 244–252, 1981.

Counselman III, C.C., and I.I. Shapiro, Miniature interferometer terminals for Earth surveying, *Bull. Geod.*, *53*, 139–163, 1979.

Davis, J.L., T.A. Herring, I.I. Shapiro, A.E.E. Rogers, and G. Elgered, Geodesy by radio interferometry: Effects of atmospheric modeling errors on estimates of baseline length, *Radio Sci.*, *20*, 1593–1607, 1985.

Davis, J.L., W.H. Prescott, J.L. Svarc, and K. Wendt, Assessment of Global Positioning System measurements for studies of crustal deformation, *J. Geophys. Res.*, *94*, 13,635–13,650, 1989.

Davis, J.L., G. Elgered, A.E. Niell, and C.E. Kuehn, Ground based measurement of gradients in the "wet" radio refractivity of air, *Radio Sci.*, *28*, 1003–1018, 1993.

Dixon, T.H., An Introduction to the Global Positioning System and some geological applications, *Rev. Geophys.*, *29*, 249–276, 1991.

Evans, A.G., and J.T. Carr, Effect of signal multipath errors at DMA Global Positioning System satellite tracking sites on orbit accuracy, *Manuscr. Geod.*, *14*, 143–148, 1989.

Genrich, J.F., and Y. Bock, Rapid resolution of crustal motion at short ranges with the Global Positioning System, *J. Geophys. Res.*, *97*, 3261–3269, 1992.

Georgiadou, Y., and A. Kleusberg, On carrier signal multipath effects in relative GPS positioning, *Manuscr. Geod.*, *13*, 172–179, 1988.

Greenspan, R.L., A.Y. Ng, J.M. Przyjemski, and J.D. Veale, Accuracy of relative positioning by interferometry with reconstructed carrier GPS: Experimental results, in *Proceedings of the 3rd International Symposium on Satellite Doppler Positioning*, pp. 1177–1195, Defense Mapping Agency and National Ocean Survey, Las Cruces, New Mexico, 1982.

Harrington, R.F., *Field Computation by Moment Methods*, Macmillan, New York, 1968.

Herring, T.A., Modeling atmospheric delays in the analysis of space geodetic data, in *Refraction of Transatmospheric Signals in Geodesy*, *Neth. Geod. Comm. Publ. Geod.*, vol. 36, edited by J.C. De Munck and T.A.T. Spoelstra, pp. 157–164, Netherland Geodetic Commission, Delft, 1992.

King, R.W., E.G. Masters, C. Rizos, A. Stolz, and J. Collins, *Surveying With Global Positioning System*, 128 pp., Dummler, Bonn, 1985.

Kraus, J.D., *Antennas*, 892 pp., McGraw-Hill, New York, 1988.

Lanyi, G., Tropospheric calibration in radio interferometry, in *Proceedings of the International Symposium on Space Techniques for Geodynamics*, edited by J. Somogyi and C. Reigber, pp. 184–195, IAG/COSPAR, Sopron, Hungary, 1984.

Leick, A., *GPS Satellite Surveying*, 352 pp., John Wiley, New York, 1990.

Liebe, H.J., An updated model for millimeter wave propagation in moist air, *Radio Sci.*, *20*, 1069–1089, 1985.

Rothacher, M., G. Beutler, W. Gurtner, E. Brockmann, and L. Mervart, Bernese GPS software version 3.4, Univ. of Bern, Switzerland, 1993.

Schupler, B.R., R.L. Allshouse, and T.A. Clark, Signal characteristics of GPS user antennas, *Navigation*, *41*, 277–295, 1994.

Spilker, J.J., GPS signal structure and performance characteristics, *J. Inst. Navig.*, *25*(2), 121–146, 1978.

Tralli, D.M., and S.M. Lichten, Stochastic estimation of tropospheric path delays in Global Positioning System geodetic measurements, *Bull. Geod.*, *64*, 127–159, 1990.

Tranquilla, J.M., Multipath and imaging problems in GPS receiver antennas, in *Proceedings of the 4th International Symposium on Satellite Positioning*, pp. 557–571, Defense Mapping Agency, Austin, Texas, 1986.

Tranquilla, J.M., S.R. Best, and B.G. Colpitts, Selection and application criteria for GPS receiver antennas, paper presented at Annual Meeting, Canadian Geophysical Union, Ottawa, Ont., May 19–21, 1986.

Tranquilla, J.M., J.P. Carr, and H.M. Al-Rizzo, Analysis of a choke ring groundplane for multipath control in Global Positioning System (GPS) applications, *IEEE Trans. Antennas Propag.*, *42*, 905–911, 1994.

Webb, F.H., and J.F. Zumberge, An Introduction to the GIPSY/OASIS-II, *JPL Publ.*, *D-11088*, 1993.

Wells, D., et al., *Guide to GPS Positioning*, Canadian GPS Associates, Fredericton, New Brunswick, 1986.

Young, L.E., R.E. Neilan, and F.R. Bletzacker, GPS Satellite Multipath: An Experimental Investigation, in *Proceedings of the First Symposium on Precise Positioning With the Global Positioning System*, pp. 423–432, National Oceanic and Atmospheric Administration, Rockville, Maryland, 1985.

J. L. Davis, P. Elósegui, and I. I. Shapiro, Harvard-Smithsonian Center for Astrophysics, 60 Garden Street, Mail Stop 42, Cambridge, MA 02138. (e-mail: elosegui@cfa.harvard.edu)

R. T. K. Jaldehag and J. M. Johansson, Onsala Space Observatory, Chalmers University of Technology, S-43992 Onsala, Sweden.

A. E. Niell, Haystack Observatory, Massachusetts Institute of Technology, Westford, MA 01886.

(Received November 11, 1994; revised March 10, 1995; accepted March 14, 1995.)